M2.8 Raman Spectroscopy

M.Turaev and M.Saravanan

August 9, 2018

Abstract

The Raman spectrum for different polarisation directions of the incident beams of Si (100) and Si (111) were obtained using a Raman spectrometer. The intensities of the Stokes lines as the function of the incident polarisation was plotted and the variation of the spectrum for different polarisations of the incident beam was studied using the Raman tensor.

Contents

1 Introduction

Raman spectroscopy works on the principle of inelastic Raman scattering in solids. This effect was first observed by Sir C.V Raman in light [1]. In this experiment we analyse the Raman spectra of the Si (silicon) crystal for different polarisation axis of the incident beam in two different directions of the crystal namely Si (001) and Si(111) directions. The phonon modes are excited by the incident laser beam and the corresponding intensities of the excitations are recorded as a spectrum by the CCDs. From the intensity of the observed phonon modes as a function of the incident polarising angle and using the Raman tensors of the crystals the symmetries of the excitations can be observed. In this lab report we will first discuss the theory that is necessary for this experiment, then we will discuss the experimental setup and how we performed the experiment. To finish off we present our analysis and results.

2 Theory

2.1 Lattice vibrations and Phonons

A crystal is made up of the periodic repetition of the unit cell in a lattice Fig. 1. In this experiment we use the Si crystal for the analysis of the Raman spectrum. The directions
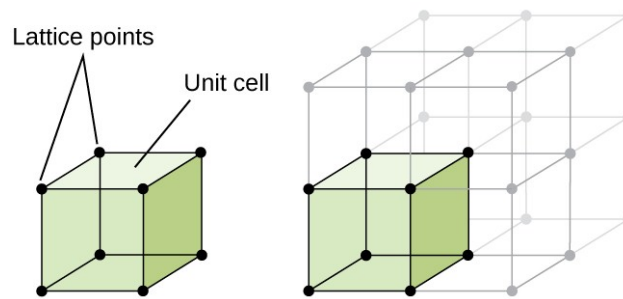

Figure 1: This figure shows the crystal in 3 dimensions. The lattice is built up by repeating the unit cell in three dimensions.

in the crystal are usually named using the miller indices, for example the x direction of the crystal is represented by (100) [2]. The crystals undergo vibrations due the other force fields. These vibrations in the crystals results in the change in the total energy of the crystal. This energy change in the crystals caused by the vibrations of the lattice points takes place in energy quanta called phonons which are analogous to the discrete energy levels in the harmonic oscillator. This excitations take place in two modes namely the optical mode and the acoustic mode. These modes correspond to the optical and acoustic phonons is whether the neighbouring atoms are in-phase or out-of-phase in their oscillations. The dispersion relations of these phonons in the reciprocal space is as shown in Fig 2. These Transverse and longitudinal vibrations are independent to each other. These modes are called as the eigenmodes and the frequency corresponding to these modes are called as the eigenfrequencies.
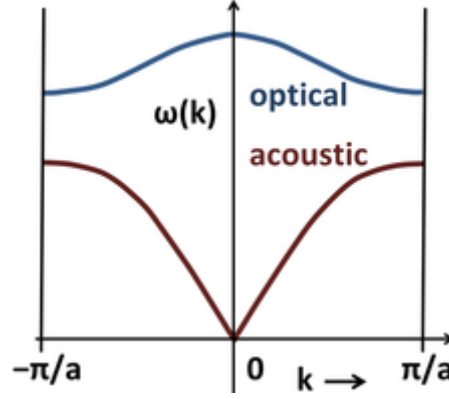
3

Figure 2: This image shows us the dispersion relation pf the phonons in the momentum state restricted to the first Brillouin zone of the crystal.

2.2 Raman effect in Solids

Raman scattering is an inelastic scattering process. In this a light beam is shined in the crystal, this light interacts with the crystal lattice and can excite the atoms in the crystal lattice which may produce a phonon. Due to this process the energy of incoming and outgoing phonons have different energies. Thus the scattered photon has energy greater or less than the incident photon this process is called as the Raman effect or the Raman scttering. This effect can be interpreted classically and quantum mechanically.

2.3 Classical Interpretation

The electromagnetic field of the incident laser beam gives an oscillating polarisation to the atoms depending on the amplitude of the oscillating electric field and the different vibrating modes of the crystal. Thus the polarisation depends upon the Electric field and a tensor quantity called the polarisability, this is given by

$$P_i = \sum_j \alpha_{ij} E_{ij} \tag{2.1}$$

Each component of the polarisability can be expanded into a series with respect to the lattice vibration q as,

$$\alpha = \alpha_0 + \frac{\partial \alpha}{\partial q} + H.O.. \tag{2.2}$$

The first term α_0 is the contribution independent of the amplitude. There is additional contribution when the polarisability change $\frac{\partial \alpha}{\partial q} \neq 0$ for an oscillating electric field of $\vec{E}(t) = E_0 \cos(\omega t)$. The polarisability becomes

$$P(t) = \alpha_0 E_0 \cos(\omega t) + \frac{1}{2} \frac{\partial \alpha}{\partial q} E_0 q_0 (\cos((\omega - \omega_1)t) + \cos((\omega + \omega_1)t)) + H.O.. \tag{2.3}$$

From this equation we can see that the out coming light has additional frequencies along with the incident frequency. We can also clearly see that there is a term corresponding to the higher frequency that give us the stokes lines and the term corresponding to the lower frequency gives us the anti-stokes lines. This is depicted in the Fig 3

For example, this process can be clearly seen in various vibrating modes of a CO_2 molecule, CO_2 has different vibrating modes as shown in the Fig 4.
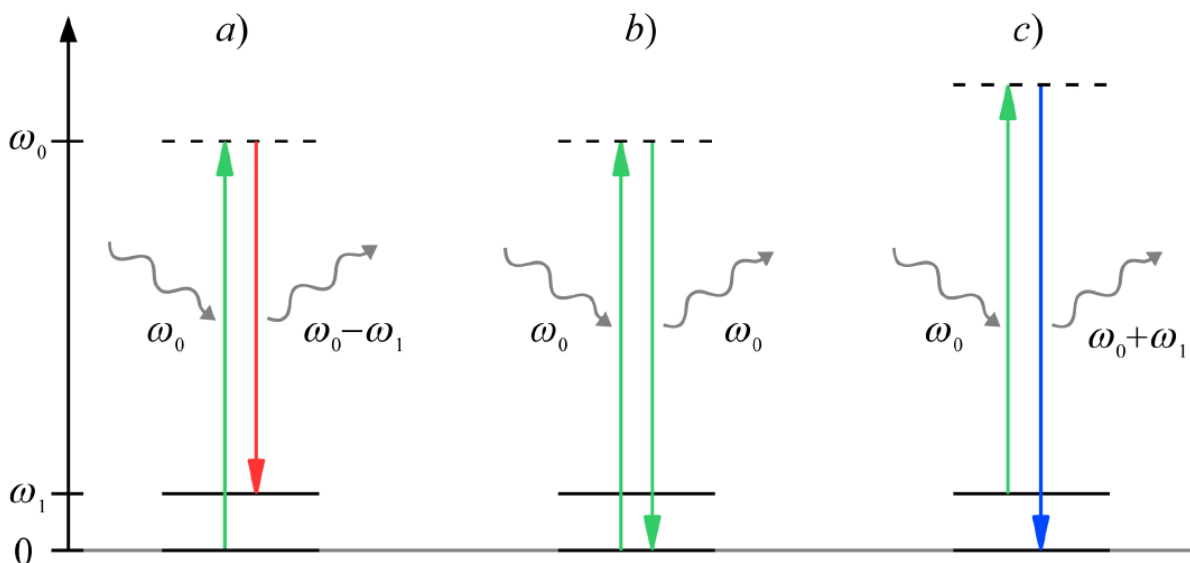
4

Figure 3: This image shows is the Raman scattering and the emission of the stokes and the anti stokes lines a) and c). Fig b) corresponds to the elastically scattered Rayleigh scattering. [3]

This molecule exhibits Raman effect only in one mode of stretching. Specifically the symmetric stretch v_1 where $\frac{\partial \alpha}{\partial q} \neq 0$ whereas the other modes give rise to Infra-red active modes where $\frac{\partial \vec{p}}{\partial q} \neq 0$.

2.4 Quantum mechanical treatment

The classical picture predicts equal intensities for both the stokes and anti stokes lines but in the spectrum at room temperature it is observed that the intensity of the anti stokes lines is less than the stokes lines. In order to understand this, a quantum mechanical picture is required. In a molecule the excitation and de-excitation taking place between the initial and the final states have to obey certain selection rules. The probability of such excitations to take place can be understood by using the Fermi's Golden rule which gives us the probability of the excitation to occur. The probability depends on the wavefunctions of the states and the matrix element as shown in (2.4). The matrix element in our case is the dipole transition matrix

$$\Gamma = |\langle \psi_f | M_{if} | \psi_i \rangle|^2 \tag{2.4}$$

The quantum mechanical picture also gives us a temperature dependence in the intensities of the observed spectrum. The probability of a excitation to occur depends on the the transition probabilities and the number of atoms in the corresponding ground state. The number of molecules in a particular state is temperature dependent. For lower temperatures, the number of molecules in ground state is almost full and hence the molecule cannot de-excite to a lower energy state hence a drop in the intensity of the anti-stokes lines. This is also the reason why the intensity of the anti-stokes lines vanishes at $0K$.
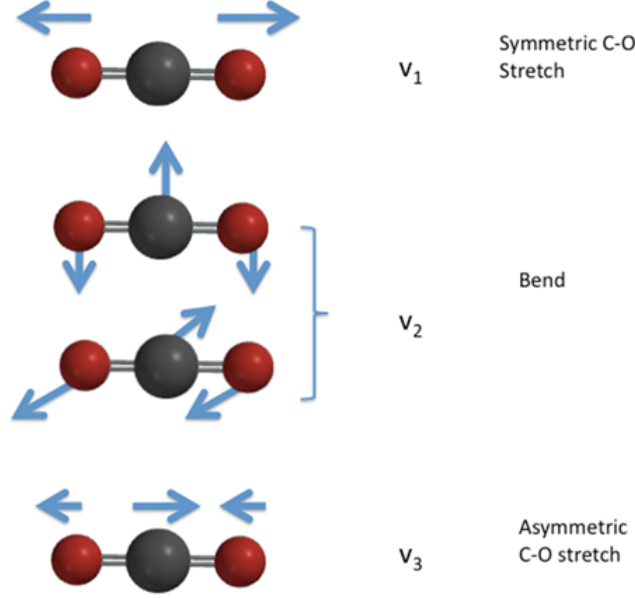
Figure 4: This image shows the different symmetry modes of stretching in a CO_2 molecule.

2.5 Raman Tensor

We have seen that the Raman lines are dependent in the direction of the crystal axes. This is usually represented in form of tensor matrices for different crystal axes. The Raman tensor depends upon the symmetry group of the particular crystal the direction of the incident beam and the direction of the outgoing beam with which the spectroscopy is done. The incoming laser beam is given as $E_{in} = (\sin\theta_{in}, \cos\theta_{in}, 0)$ and similarly $E_{out} = (\sin\theta_{out}, \cos\theta_{out}, 0)$. To make the analysis simpler we have set $\theta_{in} = \theta_{out}$. We will analyse both a Silicone (100) crystal and (111) crystal. For Si (100) the Raman tensor is given by [2]

$$\mathcal{R}_{(100)} = \begin{pmatrix} 0 & d & 0 \\ d & 0 & 0 \\ 0 & 0 & 0 \end{pmatrix} \tag{2.5}$$

The intensity can then be easily calculated as

$$I_{(100)} \propto |E_{out}\mathcal{R}_{(100)}E_{in}|^2 = d^2\sin^2(2\theta) \tag{2.6}$$

For the (111) crystal we have the following relation for the intensity

$$I_{(111)} \propto |E_{out}R^{-1}\mathcal{R}_{(100)}RE_{in}|^2 \tag{2.7}$$

where R is the rotation matrix that rotates a vector along $(0,0,1)$ into a vector along $(1,1,1)$ and is given by

$$R = \begin{pmatrix} \frac{1}{6}\left(\sqrt{3}+3\right) & \frac{1}{6}\left(\sqrt{3}-3\right) & \frac{1}{\sqrt{3}} \\ \frac{1}{6}\left(\sqrt{3}-3\right) & \frac{1}{6}\left(\sqrt{3}+3\right) & \frac{1}{\sqrt{3}} \\ -\frac{1}{\sqrt{3}} & -\frac{1}{\sqrt{3}} & \frac{1}{\sqrt{3}} \end{pmatrix} \tag{2.8}$$

6

Using this matrix we obtain the Raman tensor for the (111) orientation to be

$$\mathcal{R}_{(111)} = R^{-1} \mathcal{R}_{(100)} R = d \begin{pmatrix} -1 & 0 & 0 \\ 0 & -1 & 0 \\ 0 & 0 & 2 \end{pmatrix} \qquad (2.9)$$

Using this we obtain the intensity to be

$$I_{(111)} \propto d^2 \qquad (2.10)$$

3 Experimental Setup

3.1 Elements of the apparatus

The experimental setup consists of a laser beam, the raman signal for our crystal is expected to be at a wavelength of about $520 cm^{-1}$ [4]. So, we used a suitable laser that corresponds to the expected signal. To change the intensity of the light we use a device called the attenuator that reduces the intensity of the laser. The crystal sample we use is prepared in Si(110) and Si(111) directions and are mounted in the stand. in our experiment we analyse only the Stokes line. hence we use a filter called the edge-filter that blocks the frequencies higher than the desired frequency. The scattered light is analysed using the detector that can switch between the camera and the CCD the camera is used for the alignment and the CCD measures the spectrum the switching between the camera and the CCD id done using the computer.

3.2 Construction and Working

The sample is placed in a sample holder such that the incident beam is at about 45° to the surface of the sample. The laser beam is made to pass through attenuators and a half wave plate before hitting the sample. The light gets scattered after hitting the sample, the scattered light has a high intensity region which is blocked and a low intensity part that is made to pass through a polariser through a edge-filter before analysing using the CCD. A rough blueprint is as shown in the Fig 5

Once the experiment is setup the sample has to be mounted. for this we use a camera instead of the CCD as the CCD can burunout when a high intensity beam hits it. this switching between the CCD and the camera is done using the computer. the slit width and the crystal is adjusted such that a bright and sharp image is seen on the camera without using the edge filter. Once a proper image is achieved the edge-filter is mounted again and the light is directed back to the CCD's to get the spectrum.

4 Analysis

In this section we present the analysis and results of the measurements taken in the lab.

4.1 Fitting of the Spectrum

The spectra obtained from the spectroscopy is shown in Fig. 6. The first thing that we want to do is find a good fit for the data. The obvious choices for fitting a spectrum peak
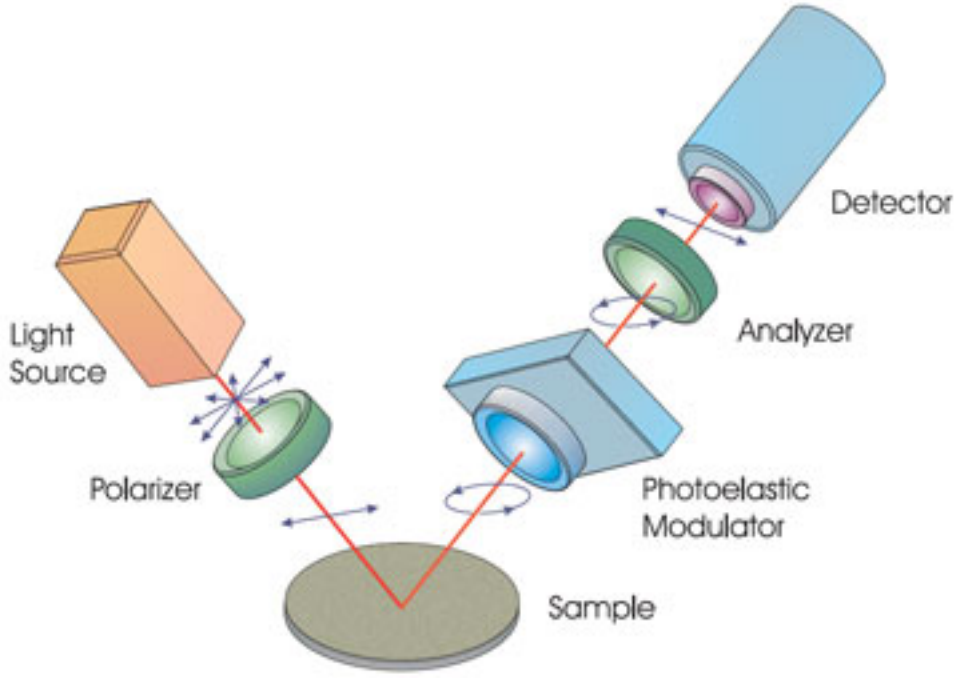
Figure 5: This image gives the basic blueprint of the experimental setup. [?]

is to use the Lorentzian function, Gaussian function or a combination of the two. For the Lorentzian fit we fitted the data to the function

$$L(x) = \frac{C}{1 + \left(\dfrac{x - x_c}{B}\right)^2} + L_0 \tag{4.1}$$

where the parameters to be fitted are C, x_c, B and L_0 For the Gaussian fit we fitted the data to the function

$$G(x) = De^{-\frac{(x - x_c)^2}{2\sigma^2}} + G_0 \tag{4.2}$$

where the parameters to be fitted are D, x_c, σ and G_0 When we considered a combination of the two the function was

$$V(x) = \alpha \frac{C}{1 + \left(\dfrac{x - x_c}{B}\right)^2} + (1 - \alpha)De^{-\frac{(x - x_c)^2}{2B^2}} + V_0 \tag{4.3}$$

where α, C, x_c, B, D and V_0 are the fitting parameters.

As we can see from the figures, the Gaussian fit is the worst of the three. The Lorentzian fit and the Combination fit both have their own drawbacks. The Lorentzian fit overestimates the peak height, but fits the background noise near the base quite well. Whereas the Combination fit underestimates the background noise, but fits the peak height quite well. Looking at table 1 we can see that the peak height predictions of the combination fit and the Lorentzian fit are very close to each other. Note: The peak height for the combination fit is given by

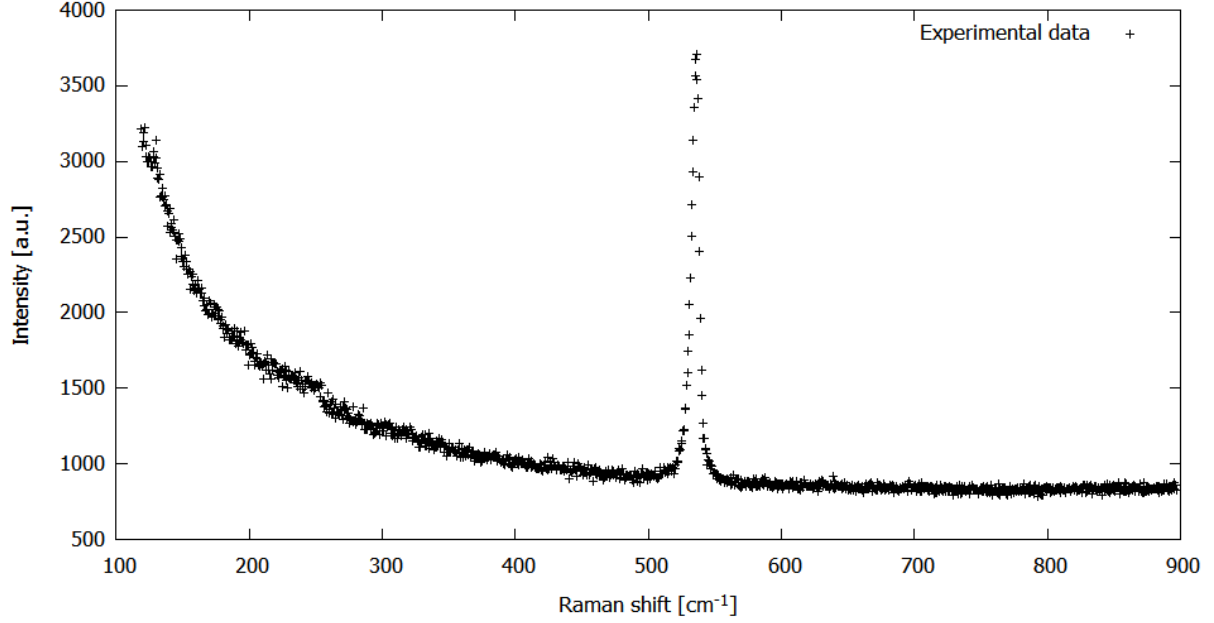$$V(x_c) = C\alpha + (1 - \alpha)D = 2922 \pm 349 \tag{4.4}$$

Figure 6: Spectrum of Silicone (100) with polarisation angle $\theta = 0$.

$G(x)$ parameters	D	x_c	σ	G_0
Values	2624 ± 51	535.27 ± 0.07	3.07 ± 0.07	985 ± 16
$L(x)$ parameters	C	x_c	B	L_0
Values	2945 ± 63	535.41 ± 0.07	3.20 ± 0.11	853 ± 21
$V(x)$ parameters	C	x_c	B	
Values	2840 ± 51	535.191 ± 0.18	3.63 ± 0.08	
$V(x)$ parameters	D	α	V_0	
Values	3232 ± 213	0.79 ± 0.05	815 ± 14	

Table 1: Table of the fitting parameters for different fits of the peak in the spectrum.

where the error was obtained by error propagation from the errors of the individual fitting parameters. We can see that the peak height of the Lorentzian fit $L(x_c) = 2840 \pm 51$ is within the range of the peak of the combination fit peak height, and also that it has a much smaller error range. Due to this and the fact that the Lorentzian fit fits the background better than the combination fit we will use Lorentzian fits for all the spectra to obtain the peak height data.

4.2   Intensity for Si (100)

Now that we have seen how we obtain the fitting parameters we will use them to analyse the intensity with the polarisation angle. We took 18 intensity readings with increments in the angle of 10°.
Fig. 8 shows the data with a fitting of the following form

$$y(x) = A \sin\left(\frac{\pi}{180} w(x - x_c)\right)^2 \tag{4.5}$$

where the fittings parameters are A, w and x_c. Because of the fact that we used half wave
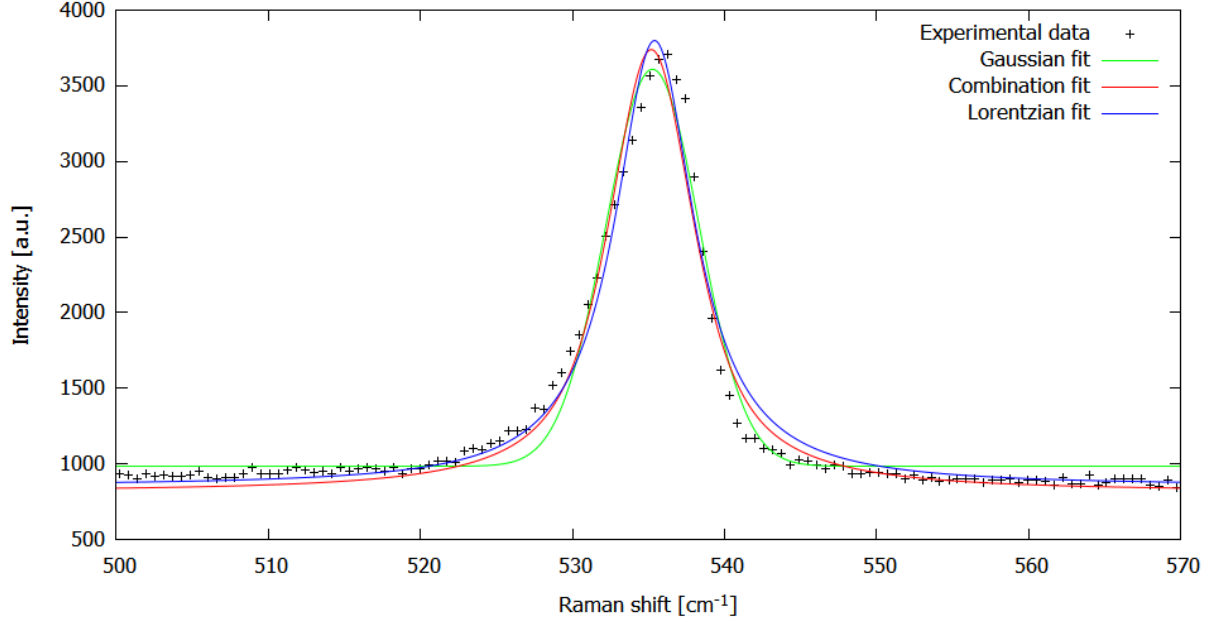
9

Figure 7: Zoomed in version of the spectrum of Silicone (100) at the peak, with different fittings for the data.

$y(x)$ parameters	A	w	x_c
Values	3200 ± 79	4.05 ± 0.04	-20 ± 1.2

Table 2: Fitting parameters of the sin squared fit of the peak height with respect to the angle.

plates in our experimental setup when we rotate by θ the real rotation is given by 2θ, therefore we expect the fit to have a $\sin(4\theta)^2$ dependence, which agrees very well with the fitting parameter w.
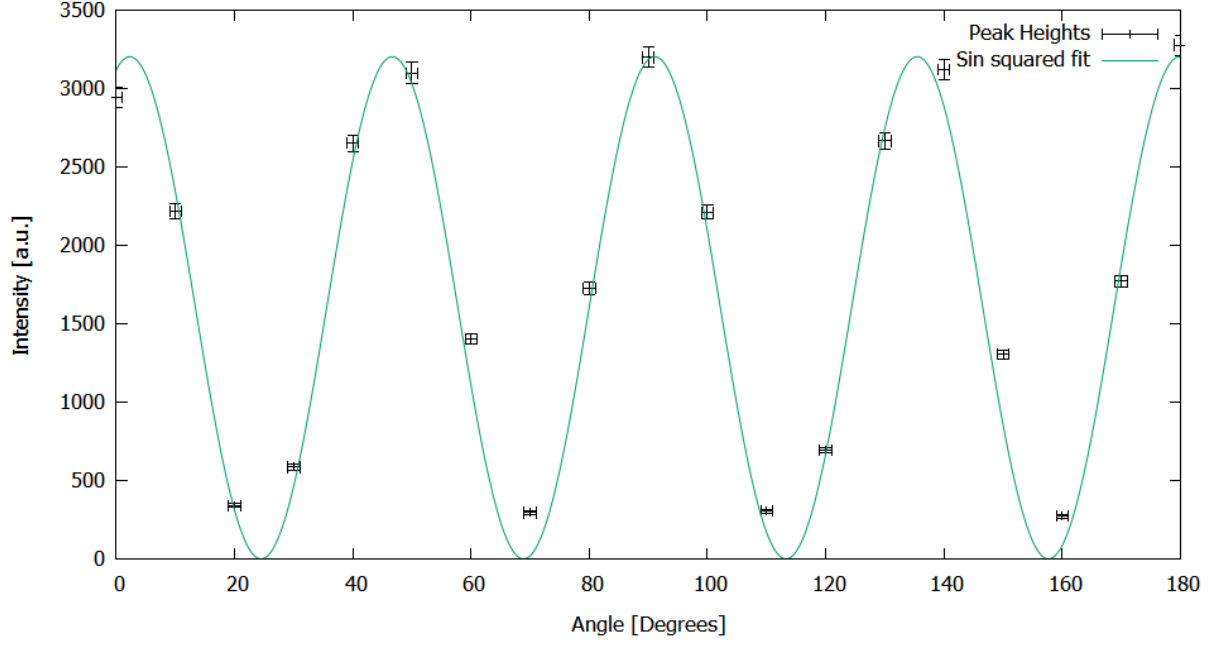
Figure 8: The peak heights against the angle. The data follows a sin squared fit.

4.3 Intensity for Si (111)

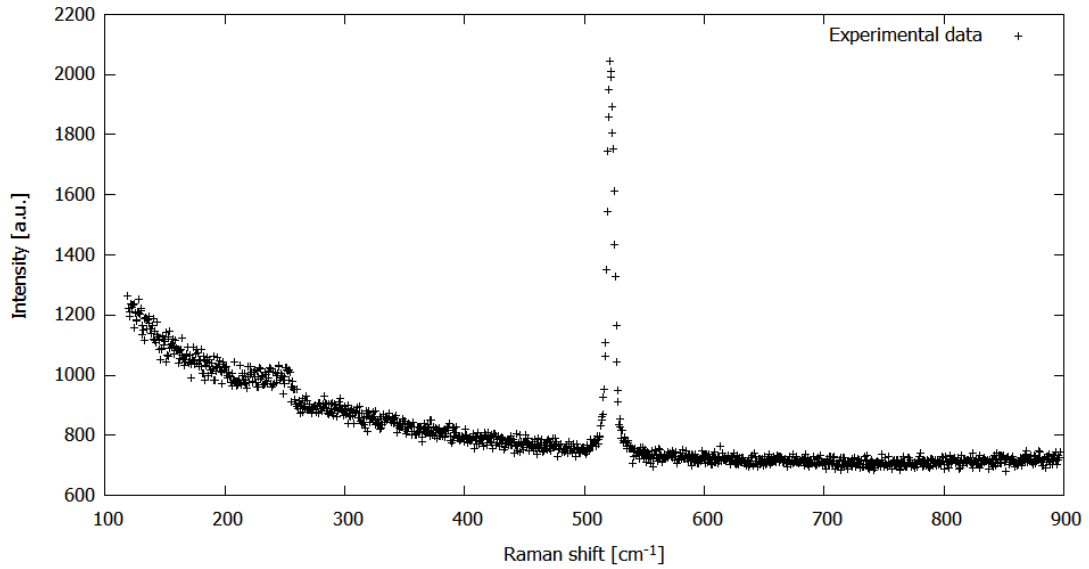For the (111) orientation we perform an analogous analysis. The spectrum is shown in Fig. 9

Figure 9: Spectrum of Silicone (111) with polarisation angle $\theta = 180$.

Once again we will use Lorentzian peaks to fit the peak. We are expecting a peak at around $520\mathrm{cm}^{-1}$[4], which can be easily seen to be the case in Fig. 9. Fig. 11 shows the data with a fitting of the following form
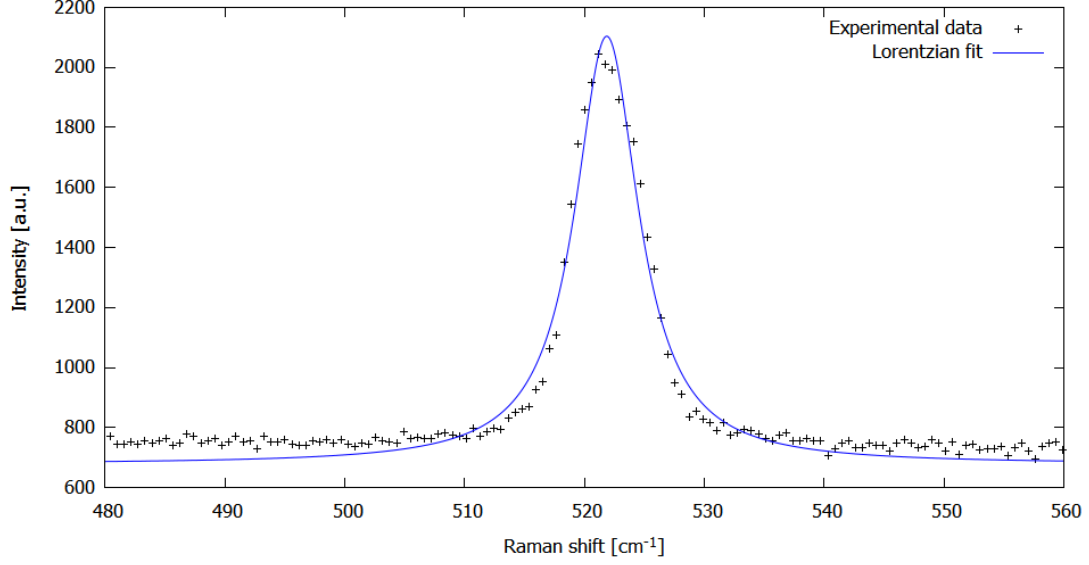
$$y(x) = y_0 \tag{4.6}$$

11

Figure 10: Zoomed in version of the spectrum of Silicone (111) at the peak, with a Lorentzian fitting for the data.
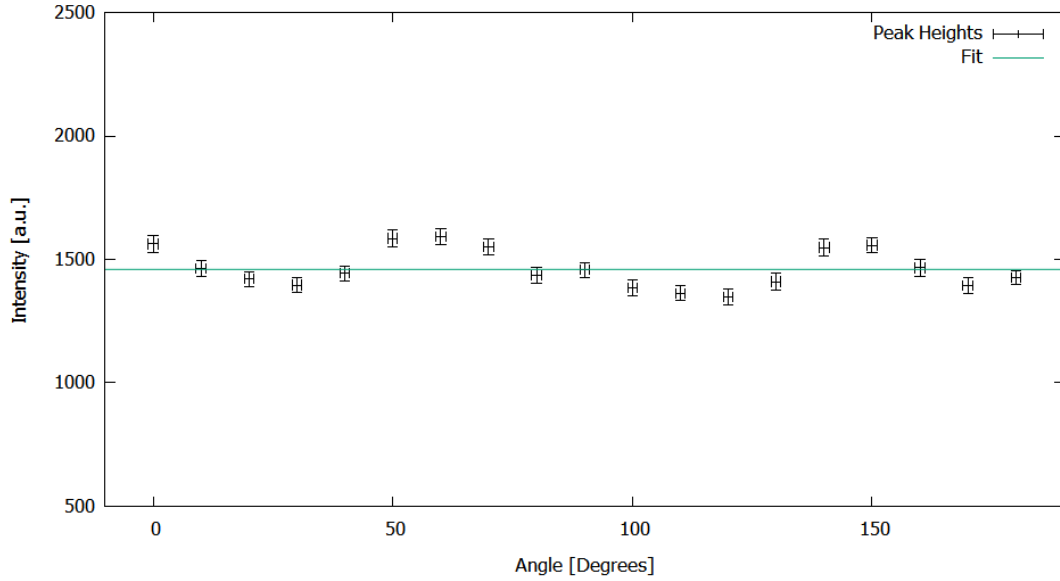

Figure 11: The peak heights against the angle.

where the fittings parameters are y_0. This fit is predicted from eq (2.10). We obtain that $y_0 = 1460 \pm 18$. As we can see we have quite a lot of fluctuation in the data, and the fit does not seem to agree too well which can also be see in Fig. 11. These fluctuations also seem regular, this might be the result of the higher order oscillations of the interaction between the light and the crystal.

5 Conclusion

In this lab report we present our measurements of the intensity dependence of the angle of polarisations of the incident light for different orientation of silicon, specifically Si

(100) and Si (111). We have used Lorentzian functions to fit the spectra and obtain the maximum intensity for different angles of the polarisation. For the Si (100) orientation the expected result is a $\sin(wx)^2$ dependence which has been realised well for $w = 4$. For the Si (111) the expected result is to be constant, but there is some fluctuation in the peak heights, so the fit was not as good as in the Si (100) measurement.

References

[1] W. A. P. Luck, Practical Raman Spectroscopy (1989), Berichte der Bunsengesellschaft für physikalische Chemie, doi:10.1002/bbpc.19900940938

[2] D.A. Long, Raman spectroscopy (1977), McGraw-Hill International Book Company, doi:10.1002/0470845767

[3] Script, Practical course M 2.8 Raman Spectroscopy. Aug 9,2012.

[4] Borowicz, Pawe & Latek, Mariusz & Rzodkiewicz, Witold & Laszcz, A & Czerwinski, Andrzej & Ratajczak, J. (2012). 3. 45003-7. doi:10.1088/2043-6262/3/4/045003.